

On the Kinematic Dynamo Action by ABC Flows

S. B. F. Dorch*

The Royal Swedish Academy of Sciences,
Stockholm Observatory,
SE-133 36 Saltsjöbaden, Sweden

PACS: 52.30.-q, 52.30.Jb, 95.30.Qd, 96.50.Bh, 96.60.Qc, 97.10.Jb

Abstract

The kinematic induction equation of MHD is solved numerically using a staggered mesh in the case of the normal ‘111’ ABC flow. Basic integral properties such as the growth rate of magnetic energy agree with previous findings, but careful 3D visualizations of the topology of the magnetic field reveal, however, that the conclusions about the modes of operation of this kinematic dynamo must be revised. The two known windows of dynamo action at low and high magnetic Reynolds number, correspond to two distinct modes, both relying on the replenishing of the magnetic field near the β type stagnation points in the flow. The results support the case for the normal ABC flow as a fast dynamo.

1 Introduction

The class of steady velocity flows called ABC flows (after Arnold, Beltrami, and Childress) is an example of how complex flows may be able to amplify weak seed magnetic fields. ABC flows have been studied in e.g. the context of the cyclonic α -effect by [1], but the main reason that this rather special type of flow is interesting to dynamo theory, is that it on the one hand constitutes a situation so simple that it is possible to understand the details of the amplification process, and that it on the other hand displays a behavior that in some respect resembles that of astrophysical dynamos such as the Sun: The amplification is related to the stretching, twisting and folding of

*E-mail address: dorch@astro.su.se

magnetic field lines, and the rôle played by the finite diffusivity is as essential to the amplification process as it is believed to be for the Sun. The main purpose of this paper is to illustrate the principle of operation of a dynamo by means of visualizing the 3-D structure of magnetic field lines and their dynamics. Doing so we discover yet unknown properties of this type of dynamo.

2 ABC Flows

The ABC flow is a 3-D periodic, incompressible and steady flow given by the sum of three parameterized Beltrami waves [2]:

$$\mathbf{u} = A(0, \sin kx, \cos kx) + B(\cos ky, 0, \sin ky) + C(\sin kz, \cos kz, 0). \quad (1)$$

Traditionally the approach is purely kinematic, so that the back-reaction in the equation of motion by the Lorentz force is ignored in the treatment (but see [3]). Thus the problem reduces to one of solving the induction equation,

$$\frac{\partial \mathbf{B}}{\partial t} = -\nabla \times (\mathbf{u} \times \mathbf{B}) + \eta \nabla^2 \mathbf{B}, \quad (2)$$

where \mathbf{B} is the magnetic field, \mathbf{u} is the velocity field (Eq. 1) and η is the magnetic diffusivity.

2.1 Method

The induction equation is solved with a simplified version of the code by Galsgaard, Nordlund and others (e.g. [4] and [5]), using both uniform magnetic resistivity and the quenched diffusion that is normally used in the full version of this MHD code: In both cases the magnetic Reynold number Re_m increases with the size of the grid as n^2 (where the number of grid points is n^3). In this paper only results from cases with constant and uniform diffusion are presented.

The induction equation is solved on a periodic finite difference staggered mesh with 6th order staggering operators, 5th order centering operators, and a 3rd order Hyman time stepping routine.

Even though the flow is steady, in certain regions of the flow trace particles follow chaotic paths so that any two trace particles separate exponentially with time — a property that has been shown to be essential for dynamo action ([6]). By varying the basic parameters of the flow A , B , C ,

and the wavenumber k it turns out that a lot of both quantitatively as well as qualitatively different topologies are possible: A special case with $A = 0$ is the G. O. Roberts dynamo used in the context of the Earth’s dynamo ([7]). While the *normal* ABC flow with $A = B = C = 1$ (hence also called the “111” flow) has 8 stagnation points, a flow with $A = 5$ and $B = C = 2$ has no stagnation points. If all the parameters are non-zero the flow in general contains a mixture of chaotic and regular islands ([8]).

The normal ABC flow has two regimes of dynamo action: One at comparatively low magnetic Reynolds numbers $\text{Re}_m = 8.5 - 17.5$ ([9]) and one starting at $\text{Re}_m \approx 27$ ([10] and [11]).

To initialize the mode in the high Re_m regime one may use a weak uniform magnetic seed field pointing in any direction. By flux conservation the uniform part remains constant, and thus rapidly becomes insignificant relative to the growing mode. To initialize the growing mode in the low Re_m window, one may use the following periodic initial condition (see [8] and [12]),

$$\mathbf{B} = (\sin(kz) - \cos(ky), \sin(kx) - \cos(kz), \sin(ky) - \cos(kx)), \quad (3)$$

which is an eigenmode of Eq. 2 in the case of zero diffusivity $\eta = 0$ and is related to the rate of strain matrix $\partial u_i / \partial x_j$ of the ABC flow.

2.2 Topology

The normal “111” ABC flow has 8 stagnation points and 8 points where the velocity is maximum (see Figure 1). A stagnation point is a point where the fluid velocity vanishes, and since the vorticity is aligned with the velocity vectors for Beltrami waves ([13]), the vorticity also vanishes at stagnation points. There are two different types of stagnation points for the normal ABC flow:

- α type stagnation points where stream lines are diverging along an axis through the stagnation point and converging in the plane perpendicular to the axis.
- β type stagnation point where stream lines are converging along the axis and diverging in the plane.

The stream lines of the flow have a three-fold symmetry in the converging (diverging) planes through the α (β) type stagnation points (see Figure 1). The three-fold symmetric ‘leaves’ of the converging/diverging stream lines

are separated by convergence/divergence connect to other stagnation points: While the separator lines and leaves of diverging stream lines of a β point connect to three α type stagnation points the reverse is true for an α point.

In itself it is not so important that there happens to be 8 stagnation points in the normal ABC flow. After all, many interesting flows do not possess stagnation points (such e.g. the flow, see [14] and turbulent flows in general), and in any case a stagnation point may be removed by a simple translation of the coordinate system. Rather it is the stretching ability of the flow that is relevant for the dynamo action. For a divergence free flow $\nabla \cdot \mathbf{u} = 0$ such as the ABC flow the induction equation may be written in the form

$$\frac{\partial \mathbf{B}}{\partial t} + \mathbf{u} \cdot \nabla \mathbf{B} = \mathbf{B} \cdot \nabla \mathbf{u} + \eta \nabla^2 \mathbf{B} \quad (4)$$

Apart from diffusive effects the stretching term $\mathbf{B} \cdot \nabla \mathbf{u}$ implies a linear growth of the logarithm of the magnetic field magnitude.

In the high degree of symmetry of the normal ABC flow the stagnation points coincide with local extrema of the stretching rate. Hence the two types of stagnation points may be seen as convenient markers of these regions.

3 Results

Below the results of experiments with normal ABC flows are divided into results concerning the growth of e.g. magnetic energy and exponential growth rates and results related to the formation and evolution of magnetic structures.

3.1 Magnetic energy

As shown in Figure 2, the initially weak seed field is indeed amplified in an exponential manner, and the growth increases with Re_m . For intermediate Re_m (in the second window), an oscillating behavior is associated with the growth (as also seen by e.g. [11], [3] and [15]), see Figure 2. The oscillation may be understood as a direct consequence of the spatial periodicity of the ABC flow ([3]). The period of the oscillation increases with increasing Re_m until a transition to a non-oscillating regime occurs at a Re_m of about 200 ([16]). Figure 2 shows examples from all three Re_m regimes.

As mentioned by [12] and [8] it is possible to rig the initial condition of the seed magnetic field such that only one mode is present in the calculations;

the special initial condition for which that is possible is given by Eq. 3.

In that case the magnetic field is not amplified in the second window as mentioned by [12]. [8] used this initial condition together with the so called ‘flux conjecture’ to try to deduce the limiting growth rate of the ABC flow. They found exponential growth of the flux in a selected region. The growth rate derived does not, however, agree with the asymptotic growth rates found by [12] and [16]. One should indeed not expect to be able to recover the growth rate of a completely different (exponentially growing) mode by studying the stretching of field lines in a another (secularly decaying) mode.

Figure 3 shows that the mode in the case of the initial condition given by Eq. 3 is an exponentially decaying mode: The decay is associated with an oscillation with a period about 10 times smaller than that of the growing mode. Because of numerical round-off errors the amplitude of the growing mode is not identically equal to zero in the initial condition, and eventually its inevitable growth and the decay of the initialized mode results in a transition from decay to growth of the total magnetic energy (see Figure 3). [12] found no growing solution and they concluded that “something odd is going on”.

3.2 Flux cigars

When the induction equation is evolved from a weak, uniform seed field, flux “cigars” rapidly arise at four of the eight stagnation points — the α -points (see Figure 4). These are the regions in the flow where the magnetic field is most rapidly advected by a converging flow in two of the three dimensions. The flux cigars are aligned along the axis of divergence through the α type stagnation points and point directly to the β type stagnation points. The regions around the β type stagnation points are not unstable to flux cigar generation since the flow there is diverging in two directions. However, the converging flow along the axis from the α points creates weaker, sheet like flux concentrations on both sides of the plane of divergence (see Figure 8).

The four flux cigars seen in Figure 4 correspond to the fastest growing eigenmode in the diffusion-less case $\eta = 0$. Initially several modes may be present but eventually the one with the largest exponential growth rate will be the only one that remains in the solution.

In our experiments we do indeed find that a second set of flux cigars is formed next to the 4 primary cigars, but we conclude that rather than obscuring the physics, they are absolutely essential. These secondary cigars have the opposite polarity of the neighboring cigars, and they are connected

by reconnecting field lines (see Figure 5).

The secondary flux cigars arise after the initial transient phase. These cigars begin to form at the α point at the separator line next to the primary cigar. As the secondary cigar forms the primary cigar moves slightly away from the center of the stagnation point. In the simulation within the oscillatory regime, as the energy increases at the beginning of a ‘cycle’, the secondary cigar increases in size and field strength until the two cigars become equal in size midway through the cycle (Figure 6). The primary cigar now becomes smaller and actually vanishes at the end of the cycle, at which time the growth of the energy slows down, and even reverses briefly. At that point the flux cigar that was previously the secondary cigar moves into the center of the stagnation point (see the evolution in Figure 6).

3.3 A dynamical amplification process

The dynamical picture of an amplification cycle may be sketched as follows in the intermediate- Re_m oscillating regime (see e.g. the case of $\text{Re}_m = 40$ in Figure 2):

In the beginning of a cycle, at one of the local minima in the magnetic energy, there is only one flux cigar at each α point (see Figure 6). Gradually field lines of the opposite polarity pile up at the separator line close to the α point where a secondary cigar will eventually form. These field lines come from the plane of divergence of a neighboring β point and are transported along two sets of converging stream lines on opposite sides of the separator line. The stream lines come from two leaves of diverging stream lines at the β point separated by the separator line: Where the stream lines reach the α point they have twisted so that the field lines they carry are parallel to the axis of divergence through the α point. At the other side of the α point one of the leaves of diverging stream lines from a β point supply field lines of the opposite polarity to the primary flux cigar. While these two flux cigars with opposite polarity sit at the stagnation point and receive field lines, the field lines that they are made of may reconnect because of their opposite polarities (see in Figure 5), and the non-vanishing magnetic diffusivity. This reconnection process is essential to the operation of the dynamo. If there were no reconnections of field lines, the magnetic field near the β points could not be replenished. It is replenished by tight field line ‘hooks’ that are released to move out along the axis of divergence through the α point towards the plane of the β point. The field lines of the legs of these hooks that come from the primary cigar are stretched out into triangular shapes

by the three-fold symmetric diverging stream lines in the plane of a β point (see Figure 7). The field lines in this leg of the hook go through the plane of divergence of the β point and connect the two primary cigars on each side of the plane. The part of the field line that makes up the bases of the triangle line up perpendicular to the separator lines and are added to the two flux cigars at the α , points at the end of these lines. The corners of the triangle are also added to α points but through the diverging leaves of the β point, that become the converging leaves of three other α points. In the plane of the β points an intricate folding of field lines takes place: Figure 8 shows isosurfaces of weak magnetic field and field lines near the plane of a β point. The plane actually constitutes a region of discontinuity where the field lines change direction from above to below.

Towards the end of a cycle, the primary cigar begins to decay, because the supply of flux to the primary cigar is less than that to the secondary cigar. At the end of one cycle the secondary cigar is the only remaining one and it moves to the center of the stagnation point.

The magnetic energy grows through most of the cycle but the main growth takes place while the two cigars have about equal sizes. This is the time at which the most rapid reconnection take place and thus the time where the largest amount of magnetic flux is released down along the axis of divergence through the α points.

The cycle discussed above is actually only a half cycle: A full cycle requires that the flux cigars return to the original polarity and this is only achieved after two of the above cycles. In this respect the ABC dynamo is similar to the solar dynamo where the full cycle of the dynamo takes two 11 year migrations of the sunspot pattern before the polarity returns to the original.

For large Re_m (in the non-oscillatory regime) the amplification process is similar to what was described above for the lower Re_m case. However, for large Re_m , there are no oscillation associated with the amplification process: The double cigars always consist of one large strong cigar and one smaller and weaker one with the opposite polarity. The secondary cigars never becomes stronger than the primary but the mechanism that drives the amplification process remains the same.

In the case of the single-cigar mode in the low Re_m window, the mode pulsates with a high frequency, corresponding roughly to the time of transport of field in a logical circle. Magnetic field of the opposite polarity to that of a pre-existing cigar is transported towards the α point by the three 'leaves' of converging flows. The three leaves do not provide equal amounts

of flux but because the diffusion is relatively large this does not result in the formation of a discrete cigar of opposite polarity. Rather, the existing cigar is surrounded from all sides by magnetic flux of opposite polarity (cf. Figure 9), its field is cancelled, and a flux cigar of opposite polarity is formed. As a result of the polarity inversion, the polarity of the magnetic flux ejected from the β point region is reversed, and the cycle repeats.

An analysis of work and dissipation shows that the average work done against the Lorentz force is positive throughout the cycle but that the average Joule dissipation is smaller than the average work in the growing phase of the cycle and larger than the average work in the decaying phase of the cycle. Averaged over a cycle, the work is slightly larger than the dissipation, and hence the mode energy grows.

4 Discussion and conclusions

The dynamo action in the two windows of Re_m correspond to two distinct modes. In both cases the replenishing of the field near the β points is crucial for the operation of the dynamo. In these regions a complicated folding of field lines takes place, that is accompanied by a discontinuity of the directions of field lines across the plane. The latter result would have been hard to discover without the use of modern visualization technics that allow direct “eye-contact” when data browsing.

Certain properties of the magnetic transport are nearly invariant as Re_m is increased: The size of the regions where diffusion is important become smaller as $Re_m^{-\frac{1}{2}}$ but reconnection still takes place and the field in the crucial β regions continues to be replenished. In the bulk of the flow where the stretching takes place the decrease of the diffusivity is unimportant since the field lines there are not influenced by diffusion: They tend to obtain a certain alignment with the flow topology given by the stretching that is an invariant property and hence the linear rate of increase of $\ln B$ remains nearly the same. It thus appears very unlikely that the double-cigar mode should go away in the limit of infinite Re_m and that the normal 111 ABC flow would not be a fast dynamo.

Acknowledgements

The author acknowledges support through an EC-TMR grant to the European Solar Magnetometry Network and thanks V. D. Archontis and Å. Nordlund for help and discussions.

References

- [1] Childress, S., *Journ. Math. Phys.* **11**, 3063 (1970).
- [2] Beltrami, E., *Opera Matematiche* **4**, 304 (1889).
- [3] Galanti, B., Sulem, P. L., and Pouquet, A., *Geophy. & Astroph. Fluid Dyn.* **66**, 183 (1992).
- [4] Galsgaard, K. and Nordlund, Å., *Journ. Geoph. Res.* **102**, 219 (1997).
- [5] Nordlund, Å, Galsgaard, K., Stein, R.F., “Solar Surface Magnetic Fields”, NATO ASI Series vol. 433 (1994).
- [6] Ott, E., “Chaos in Dynamical Systems”, (Cambridge 1993).
- [7] Rotvig, J., “The Geodynamo”, Ph.D. Thesis, (Niels Bohr Institute f. AFG 1998).
- [8] Childress, S. and Gilbert, A., *Stretch, Twist Fold: The Fast Dynamo*, (Springer 1995).
- [9] Arnold, V. and Korkina, E., *Vest. Mosk. Un. Ta. Ser. 1, Matem. Mekh.* **3**, 43 (1983).
- [10] Galloway, D. and Frisch, U., *Geophy. & Astroph. Fluid Dyn.* **29**, 13 (1984).
- [11] Galloway, D.J. and Frisch, U., *Geophy. & Astroph. Fluid Dyn.* **36**, 53 (1986).
- [12] Galloway, D.J. and O’Brian, N.R., “Solar and Planetary Dynamos”, (Cambridge University Press 1992), p. 105.
- [13] Milne-Thomson, L., “Theoretical Hydrodynamics”, (Macmillian Comp 1955).
- [14] Galloway, D.J. and Proctor, M.R.E., *Nature* **356**, 691 (1992).
- [15] Galanti, B., Pouquet, A., and Sulem, P.L., “Theory of Solar and Planetary Dynamos”, (Cambridge University Press 1993) p. 99.
- [16] Lau, Y.-T. and Finn, J.M., *Phys. Fluids B* **5**, 365 (1993).

Figure 1: A view showing the structure of the normal ABC flow: Stagnation points are marked with purple isosurfaces, regions of maximum speed with blue isosurfaces, and stream lines are white. Near the center of the view is a β type stagnation point in a plane of three-fold symmetry with diverging stream lines. In the upper right corner is an α type stagnation point connecting to the β type point via a heteroclinic orbit; along this line the velocity increases from zero to a maximum half-way, decreasing again towards zero at the β point.

Figure 2: Four panel showing the magnetic energy as function of time for the cases: $\text{Re}_m = 12, 40, 200,$ and 1600 .

Figure 3: The total magnetic energy E_M as a function of time on a logarithmic scale for two experiments (moderate Re_m) with uniform initial condition (thick line) and the initial condition given by Eq. 3 (thin line).

Figure 4: A snapshot of magnetic field strength isosurfaces at a high value (blue). Also shown are stagnation points (green) and regions of maximum speed (purple). A blue flux cigar is at a green (α type) stagnation point in the upper corner (just above the center of the picture). This cigar points towards a purple region of maximum speed, a green stagnation point (β type), yet another purple maximum speed region, and in the bottom corner is seen the opposite (periodic) end of the flux cigar.

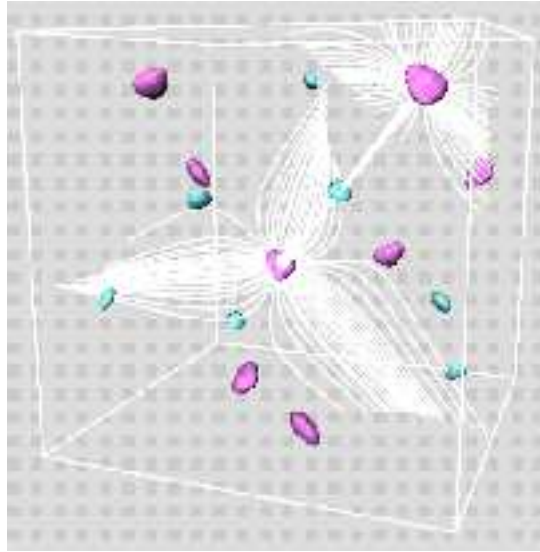
Figure 5: A snapshot from a high Re_m experiments showing the structure of the double flux cigars (transparent purple) located at an α type stagnation point, also shown are magnetic field lines in white.

Figure 6: Four snapshots (only part of the box is shown) of an experiment with a moderate Re_m showing the evolution of the double flux cigars (yellow). Also shown are converging stream lines in white and the diverging axis through the α point (in red). The four pictures correspond to four instants during the oscillation in the magnetic energy, at fractions of 0, 0.14, 0.87 and 1 of the cycle.

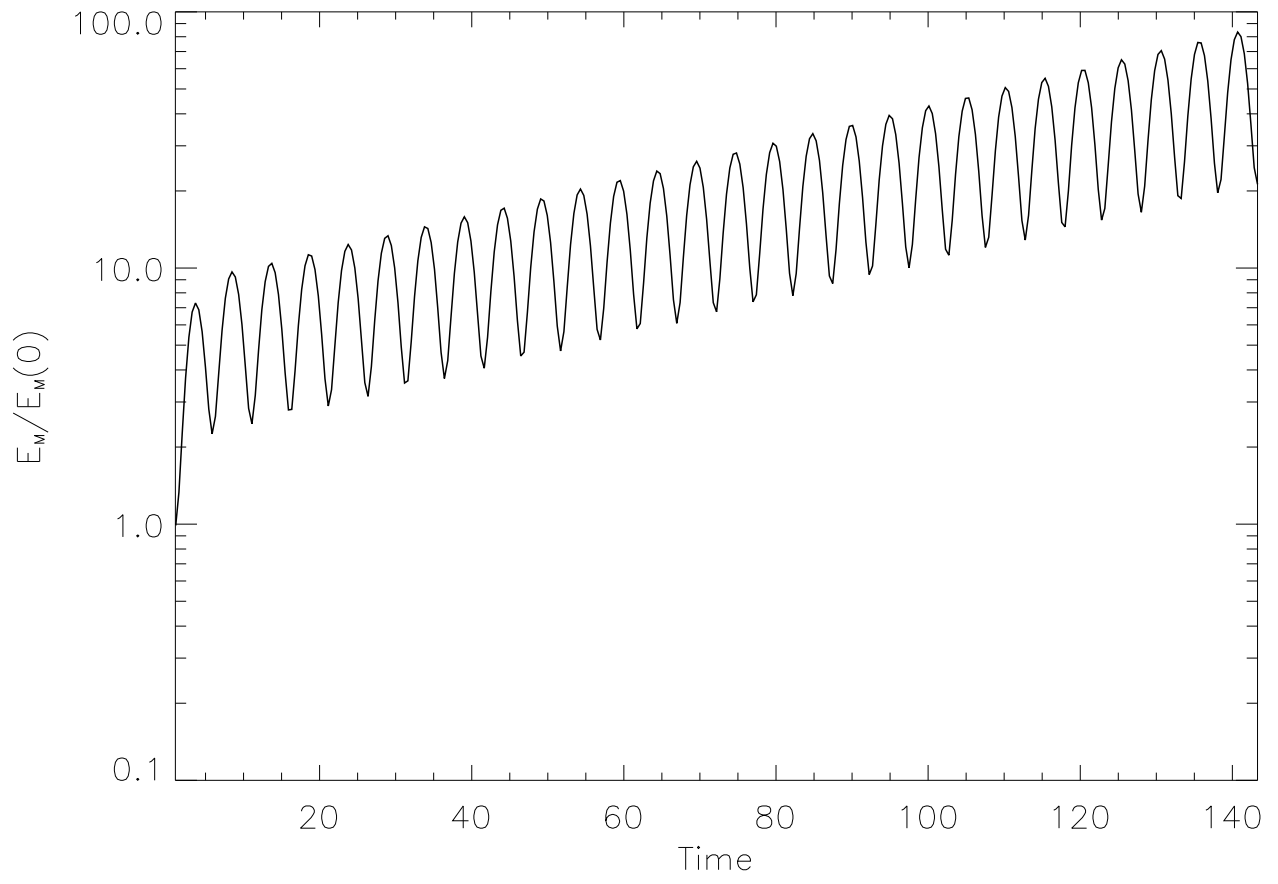
Figure 7: A snapshot from a high Re_m experiment showing double flux cigars (purple) and field lines. The black and red field lines are connected in a ‘hook’ between the double cigars in the closer corner. The field lines are stretched out in a triangle by the diverging (blue) stream lines in the plane of the β point at the center of the view.

Figure 8: A snapshot of weak magnetic field isosurfaces and field lines around a β type stagnation point. The vertical field lines near the top of the picture come from the double cigars at an α point.

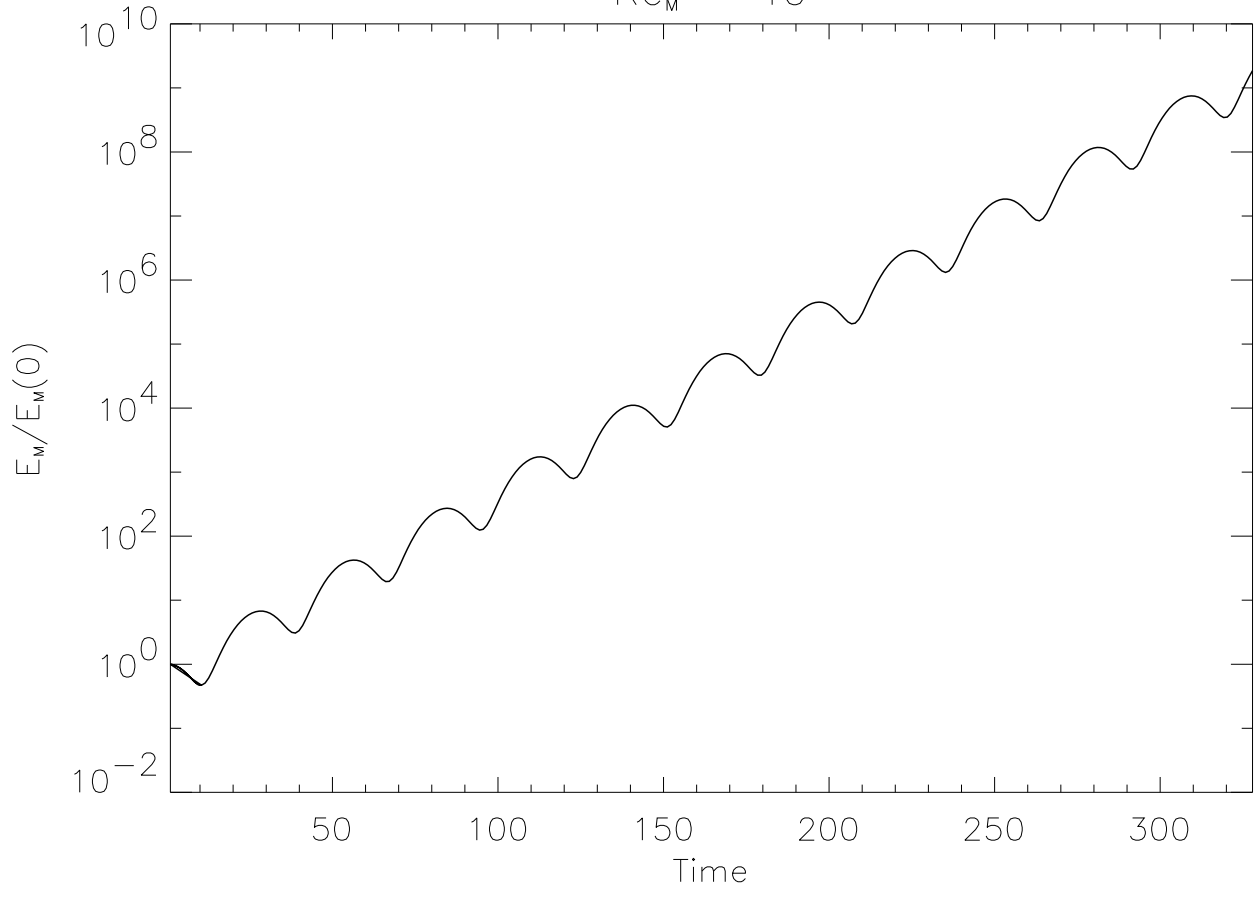
Figure 9: A snapshot from an experiments with $\text{Re}_m=12$, and the initial condition for the magnetic field given by Eq. 3 showing magnetic field lines (two sets with opposite polarity) and isosurfaces, at a time near a local minimum of magnetic energy. The flux cigar in the center is surrounded by magnetic field of opposite polarity, and Joule dissipation is high between the two polarities.



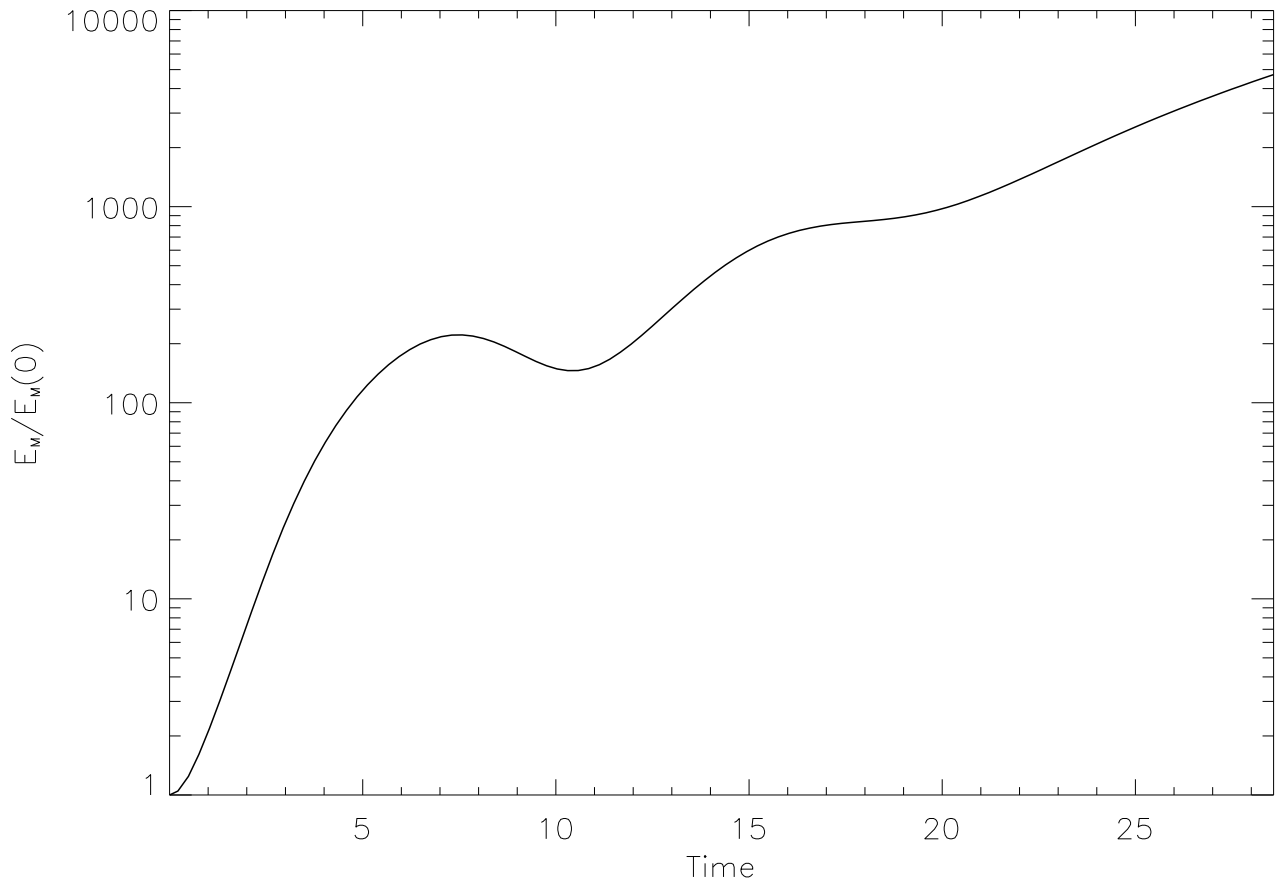
$Re_M = 12$



$Re_M = 40$



$Re_M=200$



$Re_M = 1600$

